Accepted Manuscript

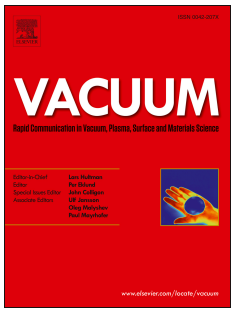

Localized deoxygenation of graphene oxide foil by ion microbeam writing

M. Cutroneo, V. Havranek, A. Mackova, P. Malinsky, L. Torrisi, J. Lorincik, J. Luxa, K. Szokolova, Z. Sofer, J. Stammers

PII: S0042-207X(18)31991-2

DOI: https://doi.org/10.1016/j.vacuum.2019.01.055

Reference: VAC 8527

To appear in: *Vacuum*

Received Date: 30 September 2018

Revised Date: 31 January 2019

Accepted Date: 31 January 2019

Please cite this article as: Cutroneo M, Havranek V, Mackova A, Malinsky P, Torrisi L, Lorincik J, Luxa J, Szokolova K, Sofer Z, Stammers J, Localized deoxygenation of graphene oxide foil by ion microbeam writing, *Vacuum* (2019), doi: https://doi.org/10.1016/j.vacuum.2019.01.055.

Localized deoxygenation of graphene oxide foil by ion microbeam writing

M. Cutroneo[1,*], V. Havranek[1], A. Mackova[1,2], P. Malinsky[1,2], L. Torrisi[3], J. Lorincik[4], J. Luxa[5], K. Szokolova[5], Z. Sofer[5], J. Stammers[1]

[1)] *Nuclear Physics Institute CAS, v.v.i., Husinec - Řež, 130, 250 68 Řež, Czech Republic*
[2)] *Department of Physics, Faculty of Science, J.E. Purkinje University, Ceske mladeze 8, Czech Republic*
[3)] *Department of Physics (MIFT), Messina University, V. le F.S. d'Alcontres 31, 98166 S. Agata, Messina, Italy*
[4)] *Research Center Rez, Hlavni 130, 25068 Husinec – Rez, Czech Republic*
[5)] *Department of Inorganic Chemistry, University of Chemistry and Technology Prague, Technická 5, 166 28 Prague 6, Czech Republic*

ABSTRACT

An efficient mask-less production of patterns in insulating foils of graphene-oxide was carried out under impact of 5 MeV alpha particle beams delivered by the Ion Micro Beam system at the Tandetron Laboratory of the Nuclear Physics Institute in Rez (Czech Republic). Graphene-oxide (GO) matrix has been exposed to controlled fluences with the aim of inducing deoxygenation and enhancement of the electrical conductivity in selected areas of the exposed samples. The reported designed patterns and their sharp edge profiles demonstrate the feasibility of the process.

The compositional changes in the exposed areas of the GO were investigated by Rutherford backscattering spectrometry, elastic recoil detection analysis, scanning electron microscopy, and correlated with the electrical properties measured by a standard 2-point probe technique.

Keywords: Ion microbeam writing, Graphene Oxide, deoxygenation, electrical conductivity

[*] Corresponding author.
E-mail address: cutroneo@ujf.cas.cz (M. Cutroneo)

1. Introduction

In the last years, graphene has attracted much attention of theoretical as well as experimental researchers due to its remarkable mechanical and electrical properties **[1, 2],** including quantum electronic transport **[3],** electron mobility **[4]** and its potential for shaping of technologies of devices such as electrodes or sensors and for energy storage. Among other graphene related materials, graphene-oxide (GO) **[5]** has risen to prominence due to its versatile functionalities. Graphene Oxide consists of hydroxyl and epoxide functional groups as basal planes and carbonyl and carboxyl groups at the edges. It is produced by the oxidation of graphite using strong oxidizing agents such as potassium permanganate. In this way, oxygenated functionalities are introduced in the graphitic planes inducing increases in interlayer spacing, lattice defects, disruption of its sp2 bonding networks and at the same time decreases the electron mobility. There are many ways in which graphene oxide can be functionalized, depending on the desired application. GO is an insulator **[6]** as it consists of oxygenated functional groups **[7]** and it exhibits conductivity of 10^{-8} S/cm. For changing the GO electrical property, chemical or heat treatments or a selective deoxygenation by ion patterning can be considered as potential routes **[8].** The patterning of graphene is often required both for investigation of its properties and for devices such as transistors, sensors, electrodes to fulfil tailored geometries and dimensions. The present work is focused on fabrication of graphene patterns by ion micro beam to enhance the possibilities for design and development of graphene-based devices. Two objectives are presented and discussed: the first one consists in the characterization of GO foils to assess the compositional changes

due to the ion irradiation, which are connected to the electrical property of GO; the other one consists in the direct patterning of graphene-oxide based on the use of suitable ion fluences. Understanding defect production in the studied substrates under ion bombardment is mandatory for their successful treatment by energetic ion beam. The radiation damage of an ion bombarded material is connected to the energy loss of the ions passing through the material. A proper tool for the simulation of the related processes is the SRIM code **[9],** which was used in our work for the estimation of the optimal irradiation conditions for the fabrication of the conductive patterns on graphene-oxide samples. The evaluation of RBS and ERDA spectra were performed by using SIMNRA 6.06 code **[10]** together with the ion beam analysis nuclear data library (IBANDL) **[11],** which provides the experimental nuclear reaction data, cross sections, and resonance parameters that are essential for reliable analyses. Graphene-oxide foil was obtained by chemical synthesizing. Then, it was irradiated by a well-controlled ion microbeam with parameters defining the ion beam stopping power, the beam current, the spot size, the exposition time, and the exposed area to produce visible micrometric pattern on the surface. The structures written in the GO samples were characterized using Scanning electron microscopy (SEM) coupled to energy dispersive X-ray (EDX) spectroscopy. The conductive nature of the pattern was evaluated by the atomic force microscopy in combination with spreading resistance imaging. The characterization of compositional changes by Rutherford backscattering spectrometry and elastic recoils detection analyses has been done by simultaneously analyzing and irradiating virgin GO foils in such a way that the

total ion fluence was the same as for ion microbeam patterned GO samples prepared for analyses by other techniques.

2. Materials and Methods

2.1. Sample preparation

Graphene-oxide (GO) foil was prepared by Hummers method using 3 g of Graphite (size grain 2–15 µm; 99.9995%; Alfa Aesar) and 2.5 g of sodium nitrate mixed with 360 ml of sulphuric acid (96 wt. %) and 40 ml of phosphoric acid (85 wt. %). Furthermore, 18 g of potassium permanganate ($KMnO_4$) were added and the mixture was heated to 50 °C over a period of 12 hours. The suspension was treated in the ice bath (400 g) with 20 mL of hydrogen peroxide (30 wt. %) to convert the residual potassium permanganate and manganese dioxide into soluble manganese sulphate ($MnSO_4$). Graphene oxide was purified by repeated sedimentation and centrifugation until negative reaction on sulfate ions (with $Ba(NO_3)_2$) was obtained. Finally, the GO suspension was frozen in liquid nitrogen and lyophilized. In the next step a suspension of GO (2.5mg/ml) was prepared using lyophilized product. A GO membrane was prepared by vacuum filtration of 20 ml of GO suspension using polycarbonate membrane (PC) with 0.45 µm micropores. The formed foil on polycarbonate membrane was dried at 50 °C for 24 hours and mechanically separated from PC membrane. A standard Mettler Toledo Micro-Balance with ± 1µg absolute accuracy was employed to evaluate the density of GO foils. Both the area and the thickness of small pieces of GO foil were evaluated using an Oxford digital microscope image analysis. For that purpose, the graphene oxide foil was fixed between two pieces of plexiglass

and then polished perpendicularly to the foil**[12]** surface. The measured average thickness was 21 µm, the thickness error was 1%, while the estimated density was 1.45 g/cm^3, with a similar error.

2.2. Sample characterization

In order to induce the effect of degradation and simultaneously evaluate the changes of physic-chemical properties of the material under ion irradiation, the ion beam analytical methods were employed. Simultaneously, Rutherford Backscattering Spectrometry (RBS) and Elastic Recoil Detection Analysis (ERDA) analyses have been performed in high vacuum (10^{-6} mbar) using 5 MeV helium beam for a period of 3500 s. After that, the differential spectra extracted after 1000 s, 2500 s and 3500 s, for periods of 500 s representing the mean deposited ion fluences of $2.3{\cdot}10^{14}$ cm^{-2}, $5.8{\cdot}10^{14}$ cm^{-2}, $8.1{\cdot}10^{14}$ cm^{-2} were analyzed. The ion current during the analyses was maintained at about 6.5 nA and the beam spot size was about (3x3) mm^2. The 5 MeV He^{2+} ions were used both for RBS and ERDA analyses as well as for the ion micro-beam patterning. The backscattered He^{2+} ions are monitored by an Ultra-Ortec PIPS silicon detector placed at 160° scattering angle. The ERDA measurement was carried out simultaneously in transmission geometry to monitor the hydrogen content in GO foil using 5.0 MeV helium ions incident at an angle of 0° degree with respect to the sample surface normal. Hydrogen atoms recoiling at an exit angle of 145° were collected at a scattering angle of 35° by a silicon detector covered with a 4 microns PP (polypropylene) foil. Both RBS and ERDA spectra were investigated using SIMNRA simulation code [10].

2.3. Sample modification

The ion microbeam writing experiment was carried out at Tandetron Laboratory of CANAM infrastructure of the NPI CAS in Rez, Czech Republic [**13**] by using an α-beam of 5 MeV energy and 260 pA current to "write a line" in a GO foil surface.

The beam of α particles passes through an analysing magnet to select mass and charge state of the incoming ions, then ions are deflected towards the beam line at + 10° **[14].** The quality of the image was ensured by focusing of the beam with the Oxford quadrupole triplet lens and by the collimation before the entrance of the target chamber, where two pairs of secondary slits adjust the spot size of the beam and reduce the effect of aberrations in the focusing system.

The beam with spot diameter of 1.5 μm was defocused to obtain spot size of 20 μm x 40 μm and then a full line of 5 mm length was drawn by moving the sample stage at constant velocity. By changing the stage velocity, three lines exposed to three different fluences were achieved: $2.8 \cdot 10^{14}$ α/cm^2 (900 nC/mm^2), $5.6 \cdot 10^{14}$ α/cm^2 (1800 nC/mm^2), $8.7 \cdot 10^{14}$ α/cm^2 (2800 nC/mm^2). A Faraday Cup was employed to monitor the beam current before and after the ion beam irradiation. Then, by knowing the exposed surface area and the exposure time the fluence could be estimated.

A software written in LabView^{TM} code**[15]** and implemented in our laboratory allowed for the patterning control of complex structures, the calculation of dose, the configuration of patterns and the scan parameters during the ion microbeam processing.

2.4. Scanning Electron Microscope (SEM)

A FIB-SEM system LYRA3 (TESCAN ORSAY HOLDING a.s.) equipped with EDX Aztec X-MAX 80 (Oxford Instruments plc) was used. The samples were analyzed at electron beam energy of 5 keV and the detectors of secondary electrons (SE) and the backscattered electrons (BSE) were used to obtain images with morphological and Z material contrast, respectively. The electron range in the GO material, assuming a density of 1.45 g/cm^3, is about 0.4 μm at 5 keV electron beam, as calculated by SREM code **[16].**

2.5. Electrical resistance measurement

The current-voltage (I-V) characteristics has been measured by the standard 2-points probe method using a Keithley 6221 current source and a Keithley 2128A nano-voltmeter. To perform electrical resistance measurement, the Ag contacts (50 nm thick) were sputtered on the surface of GO foils using a suitable mask. The change of electrical properties of GO before and after the ion irradiation at different fluences has been evaluated in the current range from -1000 nA to +1000 nA.

3. Results and Discussion

3.1. Damage and defects created by ion irradiation

In order to have an estimate of the effects induced by the interaction of He ions with the atoms of the target, the SRIM code, a semi-empirical method **[17]** based on the binary-collision approximation, has been employed.

The projected range of alpha particles with energy of 5 MeV in GO calculated using the SRIM code (assuming atomic concentrations of 46% of C, 32 % of O, 21 % of H) with 1.45 g/cm^3 density is 28.9 μm, so the He ions were not stopped inside the sample having a thickness of only 21 μm and, consequently, the Bragg

peak position is not inside the target. Therefore, virtually no nuclear collisions occur and helium ions are stopped inside the GO foil mainly due to the electronic stopping mechanism. The beam at its maximum energy at the moment of the impact exhibits electron and nuclear energy loss of S_e= 117.0 keV/μm and S_n= 79.6 eV/μm, respectively.

The He beam at its Bragg peak exhibits an electron and nuclear energy loss of the order of S_e=157 keV/μm and S_n= 2.0 keV/μm, respectively, according to SRIM Code using 100 keV helium in GO. It seems that the nuclear energy loss, which is responsible for atoms displacement, creation of collision cascades, and subsequent vacancies, can be neglected compared to the electronic one because the Bragg peak is not inside the target and no nuclear energy loss occurs.

The electronic energy loss seems to be sufficient to break the C-C (284.8 eV), C-O-C (286 eV) and the O-C=O (288.5 eV) chemical bonds and molecular chains, thus inducing subsequent dehydrogenation and deoxygenation effects in GO.

In Fig. 1, the total ion energy loss of 5 MeV of He ions irradiating a GO foil consisting of C, O, H (assuming an atomic concentration of about 46% of C, 32 % of O, 21 % of H) is plotted as a function of depth.

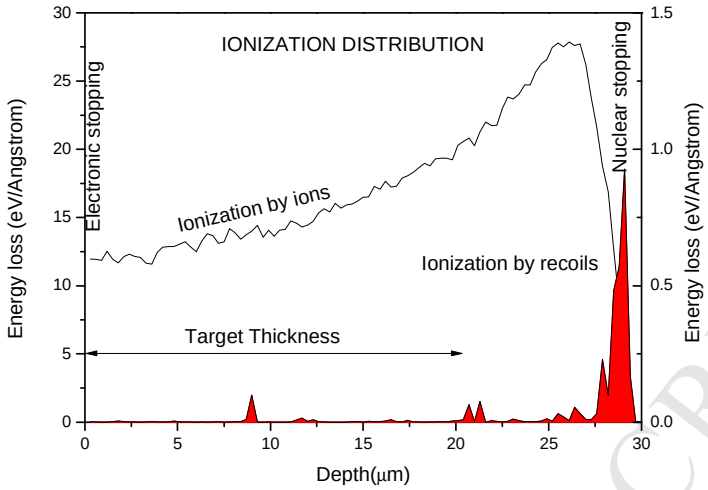

Fig. 1. SRIM simulation of the electronic and nuclear ion energy loss vs. depth of 5 MeV Helium ions irradiating a GO foil.

Due to the limited thickness of the foil of only 21 μm, the ions are stopped essentially only due to electronic stopping mechanism because the Bragg peak, at which the nuclear stopping occurs, is located at a depth of about 29 μm, i.e. outside the foil. Therefore, the defects due to nuclear collisions, consisting of vacancies, atom displacements, and collision cascades produced mainly at the Bragg peak position, are negligible.

3.2. Rutherford Backscattering Spectrometry and Elastic Recoil Detection Analysis

The RBS and ERDA analyses provided evaluation of the comparison of the atomic compositions up to ~ 1 μm depth in virgin and in GO foils implanted with 5.0 MeV He ions. The graphene oxide contains mainly carbonyl groups C=O, hydroxyl group –OH, and carboxyl groups –COOH, which can release oxygen by

chemical scissions process. The relased oxygen can then recombine and be emitted into the gaseous phase.

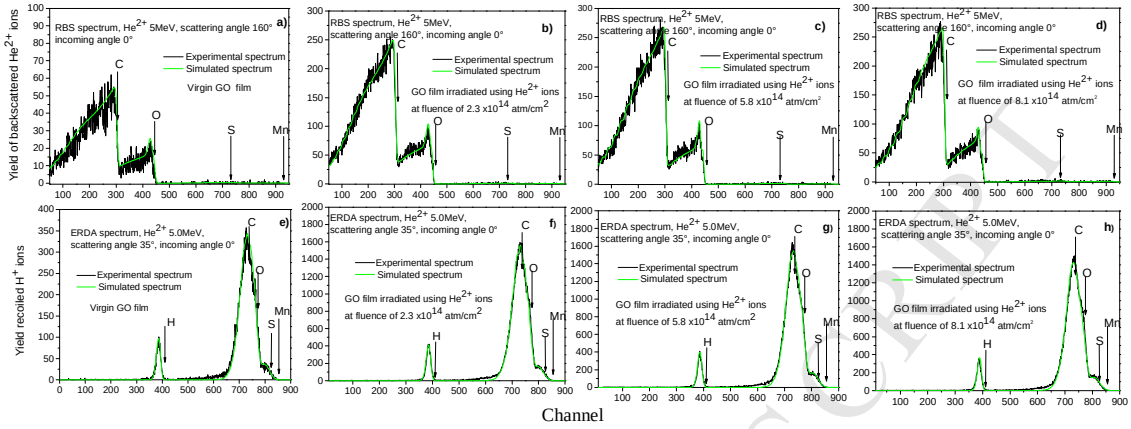

Fig. 2. RBS and ERDA spectra for GO treated by irradiation of 5.0 MeV Helium ions with 2.3 x 10^{14} ions/cm^2 a) d) 5.8 x 10^{14} ions/cm^2 b) e) and 8.1 x 10^{14} ions/cm^2 c) f) respectively.

However, also trace elements such as sulfur, and manganese, have been found in both virgin and implanted GO foils, probably due to the GO preparation procedure. Potassium, phosphorus, calcium were also expected in the sample but their concentration was below the detection limit of the employed techniques. In Fig. 2 the ERDA spectra are reported showing hydrogen concentrations of 20% after irradiation time of 1000 s (a), 19 % after 2500 s (b), and 18 % after 3500 s (c), producing final reduction of 14.3 % of hydrogen content.

The same figure reports also the RBS spectra, from which it is possible to evaluate the hydrogen/oxygen (H/O) and the C/O ratios of about 0.67 and 1.63 by implanting at a fluence of 2.3·10^{14} ions/cm^2 (d), 0.70 and 1.96 after a fluence of 5.8·10^{14} ions/cm^2 (e), and 0.72 and 2.24 after a fluence of 8.1·10^{14} ions/cm^2 (f).

The reduction of 14.3 % of hydrogen and 21.8 % of oxygen, evaluated by ERDA and RBS measurements, respectively, suggests the reduction of hydroxyl and carboxyl functional groups. The relative content of C increased to about 17.8 %, which was due to the ion irradiation of the GO foil leading to the modification of the local elemental content. The reason is that the chemical changes induced by ionizing radiation involve the creation of free radicals, the formation of chemical bonds, the formation of groups with desorption of gases. Table 1 reports the changes in composition of the GO foils.

Table 1. The elemental composition of GO foils determined by RBS and ERDA as a function of the exposed fluence

COMPOSITION OF THE GO FOILS [atm.%]					
Sample/Ions	*C*	*O*	*H*	*C/O*	*H/O*
GO Virgin	*46±0.1*	*32±0.3*	*21±0.4*	*1.44±0.003*	*0.66±0.004*
2.3 10^{14} cm^{-2}	*49±0.5*	*30±0.4*	*20*	*1.63±0.003*	*0.67±0.004*
5.8 10^{14} cm^{-2}	*53±0.2*	*27±0.2*	*19±0.1*	*1.96±0.002*	*0.70±0.003*
8.1 10^{14} cm^{-2}	*56±0.2*	*25±0.1*	*18±0.1*	*2.24*	*0.72*

Moreover, the effects of scissions and production of oxygen radicals due to the electronic stopping power were responsible for the ionization and for the modification of the structure of irradiated foils, as observed also in SEM-EDX analyses.

3.3. SEM-EDX

Scanning Electron Microscopy (SEM) and Energy Dispersive X-ray Spectroscopy (EDX) measurements were carried out to characterize the structure of the line written onto the GO foils and the relative amounts of carbon, oxygen and sulfur, respectively.

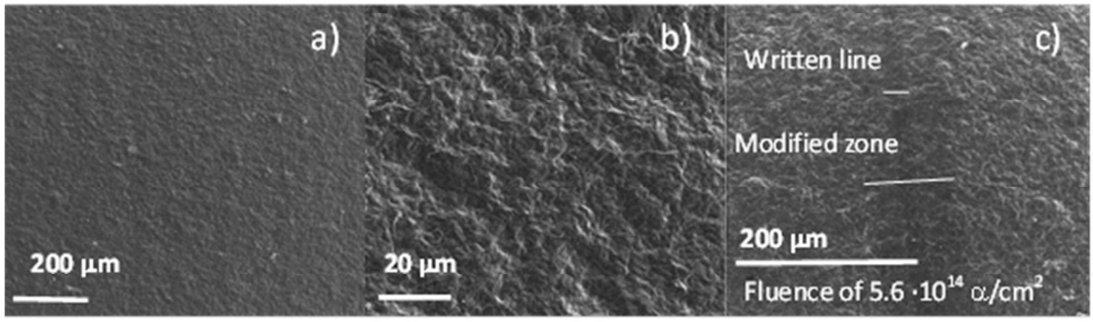

Fig. 3. SEM images at 5 keV of virgin GO foils at field of view (FOV) of 1 mm (a) and 100 μm (b), and of a GO foil at FOV 400 μm (c). The line written at a fluence of $5.6 \cdot 10^{14}$ α/cm^2 (1800 nC/mm^2) into the GO foil is clearly visible.

Fig. 3 shows the surface structure of the studied GO samples at various fields of view (FOV). In Fig. 3 (c) a vertical line of 20 μm of width written in GO foil by the micro ion beam and a broader modified area of about 100 μm width are clearly visible. That area can be due to local electrical discharges occurring during the irradiation of non-conductive areas, the production of delta rays along the ion tracks, re-deposition of carbon ions on the surface, and effects of layer relaxation.

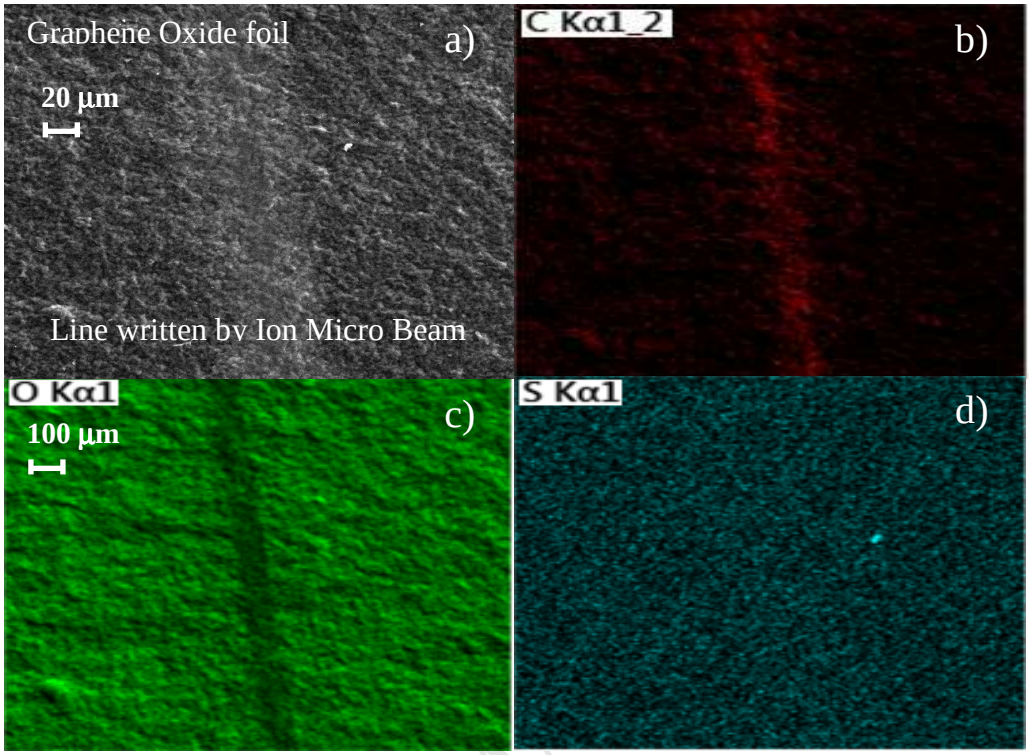

Fig. 4. SEM image of implanted line in the GO layer (a), SEM –EDX maps of C (b), O (c), and S (d).

Chemical composition of the lines and the altered areas investigated using SEM-EDX is depicted in Fig. 4. The elemental maps in Fig.4 are qualitative as the pixel brightness indicates only higher or lower signal.

The dark line in Fig. 4 c is an indication of a localized deoxygenation of the GO film after the ion bombardment. Similarly to O, the implantation line in Fig. 4 b indicates a relative enhancement of C at the surface. The trace contaminant S has been explored for comparison with RBS analysis. It appeared uniformly distributed with a minor localized enhancement.

In Fig. 5, the I-V characteristic curve is presented for virgin GO foil, GO foil irradiated at $2.86 \cdot 10^{14}$ ions/cm^2, $5.6 \cdot 10^{14}$ ions/cm^2 and $8.76 \cdot 10^{14}$ ions/cm^2 and for comparison virgin reduced GO(rGO) **[18].**

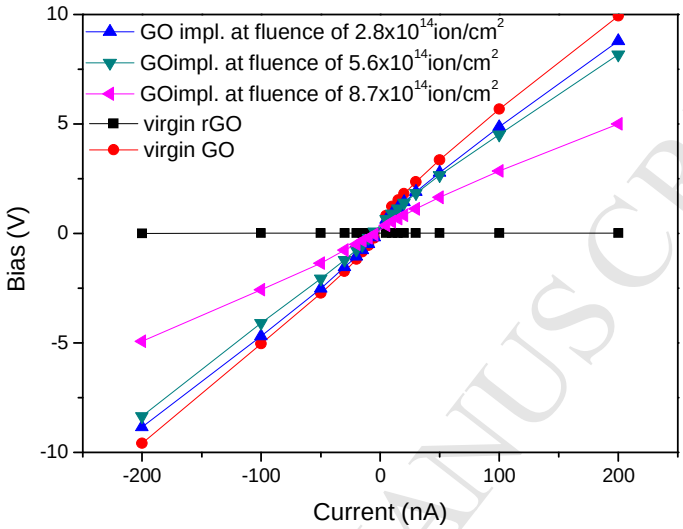

Fig. 5. I/V characteristic of virgin GO, virgin rGO and irradiated GO $2.8 \cdot 10^{14}$ ions/cm^2, $5.6 \cdot 10^{14}$ ions/cm^2 and $8.7 \cdot 10^{14}$ ions/cm^2.

The GO foil irradiated at $8.7 \cdot 10^{14}$ ions/cm^2 fluence showed lower current response than the rGO and higher compared to the pristine GO foil. The result is due to the interaction of graphene oxide with high energy ion beam, which led to the decomposition of oxygen functional groups and formation of conductive reduced graphene oxide. Removal of oxygen functional groups led to improvement of graphene oxide material conductivity.

4. Conclusions

The ion microbeam writing technique has been employed to write a line on graphene oxide foil using a 5.0 MeV helium ion beam, which lead to localised changes of compositional and electrical features. The results indicate close

relationship between the ion irradiation fluence and the element content in the GO foil. The RBS and SEM measurements are in good agreement revealing local reduction of oxygen as well as a local relative enhancement of carbon contents after the ion irradiation.

The ion microbeam writing exhibits a high control over the patterns written in a graphene based material, which can be beneficial for device fabrication **[19].** It was shown that the ion microbeam is an efficient way to deoxygenate the graphite oxide foils and produce a reduced graphene oxide to enhance the relative carbon content (C/O ratio) for increasing the electrical conductivity, as reported in literature **[20].**

The presented work is aimed at designing direct-pattern circuits and complex structures in a single step process without masks, templates, and post-processes, using a fixed ion beam in vacuum for writing patterns in thin graphene oxide foils.

Acknowledgements

The research has been carried out at the CANAM (Centre of Accelerators and Nuclear Analytical Methods) infrastructure LM 2015056 and the SUSEN infrastructure CZ.1.05/2.1.00/03.0108 (ERDF) and supported by project GACR 16-05167S, project CANAM OP,CZ.02.1.01/0.0/0.0/16_013/0001812, project LQ1603 (Research for SUSEN), the specific university research (MSMT No. 20-SVV/2017) and the Neuron Foundation for science.

References

[1] F. Traversi, F. J. Guzman-Vazquez, L. G. Rizzi, V. Russo, C. Spartaco Casari, C.Gómez-Navarro et al.,, **Elastic properties of graphene suspended on a polymer substrate by e-beam exposure,** New Journal of Physics 12(2) (2010) 023034. https://doi.org/10.1088/1367-2630/12/2/023034

[2] A. C. Neto, F. Guinea, N.M. R. Peres, K. S. Novoselov, and A. K. Geim, **The electronic properties of graphene,** Rev. Mod. Phys.81 (1) (2009) 109-162. https://doi.org/10.1103/RevModPhys.81.109

[3] K.S. Novoselov, A.K. Geim, S.V. Morozov, D. Jiang, M. I. Katsnelson, I. V. Grigorieva et al., **Two-dimensional gas of massless Dirac fermions in graphene,** Nature 438 (2005) 197-200. https://doi.org/10.1038/nature04233

[4] M. Poljak, K.I. Wang, T. Suligoj, **Variability of bandgap and carrier mobility caused by edge defects in ultra-narrow graphene nanoribbons,** Solid State Electron 108 (2015) 67-74. https://doi.org/10.1016/j.sse.2014.12.012

[5] D. A. Dikin, S. Stankovich, E. J. Zimney, R. D. Piner, G.H. Dommett, G. Evmenenko et al., **Preparation and characterization of graphene oxide paper,** Nature 448 (2007) 457-460. https://doi.org/10.1038/nature06016

[6] D. A. Dikin et al. **Preparation and characterization of graphene oxide paper,** Nature 448 (2007) 457−460. https://doi.org/.10.1038/nature06016

[7] D. R. Dreyer, S. Park, C. W. Bielawski, R. S. Ruoff, **The chemistry of graphene oxide,** Chem. Soc. Rev. 39 (2010) 228−240. https://doi.org/10.1039/b917103g

[8] D. E. Lobo, J. Fu, T. Gengenbach and M. Majumder, **Localized Deoxygenation and Direct Patterning of Graphene Oxide Films by Focused**

Ion Beams, Langmuir 28 (2012) 14815−14821. https://doi.org/10.1039/B917103G

[9] www.srim.org/

[10] M. Mayer, SIMNRA version 6.06, Max-Planck-Institut fur Plasmaphysik Garching, Germany, **2006**. http://www.rzg.mpg.de/~mam/.

[11] https://www-nds.iaea.org/ibandl/

[12] M. Cutroneo, L. Torrisi, J. Badziak et al., **Graphite oxide based targets applied in laser matter interaction**, EPJ Web of Conferences 167, 02004 (2018). https://doi.org/10.1051/epjconf/201816702004

[13] M. Cutroneo, A. Macková,V. Havranek, P. Malinsky, L. Torrisi, M. Kormunda, et al., **Ion Beam Analysis applied to laser-generated plasmas,** Journal of Instrumentation 11 (2016). https://doi.org/10.1088/1748-0221/11/04/C04011

[14]M. Cutroneo, V. Havranek, A. Mackova, V. Semian, L. Torrisi, L. Calcagno, **Micro-patterns fabrication using focused proton beam lithography,** NiM B 371 (2016) 344-349. https://doi.org/10.1016/j.nimb.2015.10.006

[15] http://sine.ni.com/nips/cds/view/p/lang/cs/nid/209015

[16] www.srim.org/SREM.htm

[17] J. F. Ziegler, M. D. Ziegler, J. P. Biersack, **SRIM-The Stopping and Range of Ions in Matter,** Nuclear Instruments and Methods in Physics Research Section B: Beam Interactions with Materials and Atoms, 268(11–12) (2010)1818-1823. https://doi.org/10.1016/j.nimb.2010.02.091

[18]G. S. Bocharov, A. V. Eletskii, V. P. Melnikov, **Electrical properties of thermally reduced graphene oxide**, Nanosystems: Physics, chemistry,

mathematics, 9(1) (2018) 98-101. https://doi.org/10.17586/2220-8054-2018-9-1-98-101

[19] D. C. Bell, M. C. Lemme , L. A. Stern , J. R. Williams, C. M. Marcus, **Precision Cutting and Patterning of Graphene With Helium Ions,** Nanotechnology 20 (45) (2009) 455301. https://doi.org/10.1088/0957-4484/20/45/455301

[20] M. Aliofkhazraei, N. Ali, W.I. Milne, C.S. Ozkan, S. Mitura and J.L. Gervasoni, **Graphene Science handbook, Electrical and optical properties,** CRC Press, Taylor & Francis, London, 2016: 750, ISBN 9781466591318 - CAT# K20507

- An ion micro beam was used for writing on graphene oxide inducing selective modification of its electronic properties in the irradiated areas.
- The compositional changes induced by the ion irradiation were investigated as a function of the ion fluence.
- Chemical changes and surface structure modifications were characterized by SEM analysis.
- The exposition to controlled fluences of alpha particles changed the properties of graphene oxide from insulator to semiconductor.
- The ion microbeam was shown to be a promising tool for local control of GO conductivity with prospects for the design and development of graphene –based electronic devices.